IEEE Access
Multidisciplinary | Rapid Review | Open Access Journal

Received February 11, 2020, accepted March 9, 2020, date of publication March 18, 2020, date of current version April 2, 2020.

Digital Object Identifier 10.1109/ACCESS.2020.2981730

HRRP Target Recognition With Deep Transfer Learning

YI WEN, LIANGCHAO SHI, XIAN YU, YUE HUANG, AND XINGHAO DING
School of Informatics, Xiamen University, Xiamen 361005, China
Key Laboratory of Sensing and Computing for Smart City, Xiamen University, Xiamen 361005, China

Corresponding author: Yue Huang (yhuang2010@xmu.edu.cn)

This work was supported in part by the National Natural Science Foundation of China under Grant 81671766, Grant 61571382, Grant U19B2031, Grant 61971369, Grant U1605252, and Grant 81671674, and in part by the Fundamental Research Funds for the Central Universities under Grant 20720180059 and Grant 20720190116.

ABSTRACT Recently, radar high-resolution range profile (HRRP) recognition based on convolutional neural networks (CNNs) has received considerable attention due to its robustness to translation and amplitude changes. Most of the existing methods require that sufficient labeled data with complete aspect angles be used as training data, which is a difficult task in practice. In addition, HRRP signals have a high sensitivity to the aspect angle. Therefore, the representative and discriminative powers of the features extracted from typical CNN models are reduced due to incomplete aspect angles in the training data, which significantly limit the recognition performance. This paper first considers the problem of HRRP recognition with incomplete aspect angle training data and addresses the problem by a deep transfer learning framework. Specifically, the two proposed methods enhance the recognition performance by exploring the discriminative power and the intraclass consistency with auxiliary data, which have HRRP signals with complete aspect angles. This paper generates a simulated HRRP dataset from public data to validate the proposed work. The comparisons of the recognition results demonstrate that the proposed framework outperforms the latest CNN-based models.

INDEX TERMS High-resolution range profile, target recognition, deep learning, transfer learning.

I. INTRODUCTION

The high-resolution range profile (HRRP) is the vector sum of the radar echo projected on the ray, as shown in Figure 1, which is the sequence of the target scattering intensity distribution [1]. Target recognition based on HRRP signals plays an important role in radar automatic target recognition (RATR) systems for the following reasons: (1) the HRRP signal contains comprehensive information, including the target's material, size, scattering information, and the electromagnetic characteristics of the target for radar-related applications; (2) compared to synthetic aperture radar (SAR) images, the HRRP is in vector form, which effectively reduces the storage capacity and computational cost; and (3) only the transmission radar wide-band signals are required to obtain the HRRP sequence [2], [3].

As a typical pattern recognition problem, feature extraction is one of the fundamental issues in HRRP recognition. Several feature extraction improvements have been reported. Liu *et al.* [4] proposed a stable dictionary learning method to solve the problems of mismatched and abnormal amplitudes between the sparse representations of similar targets in HRRP signals. Du *et al.* [5] introduced a factorized discriminative conditional variational autoencoder (FDCVAE) to improve the robustness of aspect angle feature extraction. Zhang *et al.* [6] proposed an adaptive preserved neighborhood discriminant projection method to enhance the feature extraction capability. Another challenge in HRRP signal processing is the low signal-to-noise ratio (SNR), which can reduce the recognition efficiency. To address this problem, Pan *et al.* [7] introduced an enhancement method based on a Gaussian model. Du *et al.* [8] proposed a scattering matching algorithm. Both methods solved the problem of low SNRs to a certain extent.

Recently, deep learning models have been widely used in many recognition tasks due to their strong representative power using stacked nonlinear structures [9], [10]. HRRP classification using a deep neural network has also been reported, which has the ability to extract high-order HRRP features in an automatic data-driven manner [11], [12].

The associate editor coordinating the review of this manuscript and approving it for publication was Guolong Cui.

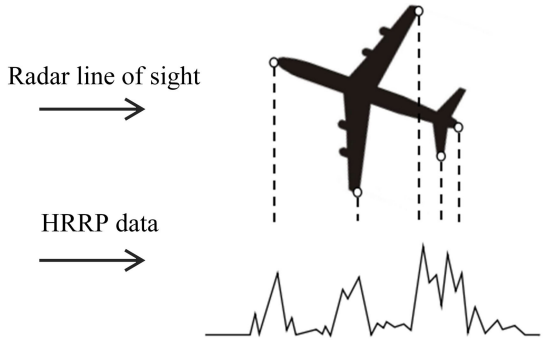

FIGURE 1. An example of HRRP signal generated from an aircraft target, the circles on the target indicate the scattering centers.

The autoencoder is one of the most widely used models. Feng *et al.* [13] proposed a stacked corrective autoencoder model called a SCAE-based multilayer nonlinear network, which is the first step in deep learning-based HRRP recognition. Xu *et al.* [14] proposed an RNN-based target-aware recurrent attentional network (TARAN), which is more robust to temporal shifts due to the memory function of the RNN and attention mechanism. Recently, convolutional neural network (CNN) models have attracted considerable attention in HRRP signal analysis by considering the sensitivity of HRRP signals. Compared with autoencoders, CNNs achieve better performance due to their robustness in terms of translation invariance and rotation invariance, which are able to ease the burden of data sensitivity of HRRP signals [15], [16]. For example, a deep network of concatenated structures [17], one-dimensional residual-inception structures [18], and a deep-u-blind denoising network (DUBDNet) [19] have been proposed to improve the recognition performance and achieve a promising recognition effect. Most of the existing works contribute to HRRP target recognition by modifying the architecture of CNN models. However, the sensitivity of HRRP signals to aspect angles is still a difficult challenge in HRRP feature extraction.

Deep learning-based HRRP recognition achieves promising performance by exploring discriminative and representative patterns in large-scale training data. As mentioned previously, HRRP signals have various signal amplitudes with different aspect angles; that is, the sensitivity to the aspect angle is significant. Figure 2 shows four subimages denoting the same target with four different aspect angles, which indicates that the variance is very large. The existing HRRP recognition method works via deep learning and always assumes that the training samples cover all the possible aspect angles to explore the discriminative patterns. However, in real-world applications, HRRP data are difficult to obtain, especially from noncooperative targets. Therefore, it is extremely difficult to collect sufficient training HRRP data with complete aspect angles, for example, 1°-180°. Thus, if the aspect angle is incomplete in the training set, both the representative and the discriminative powers of the extracted

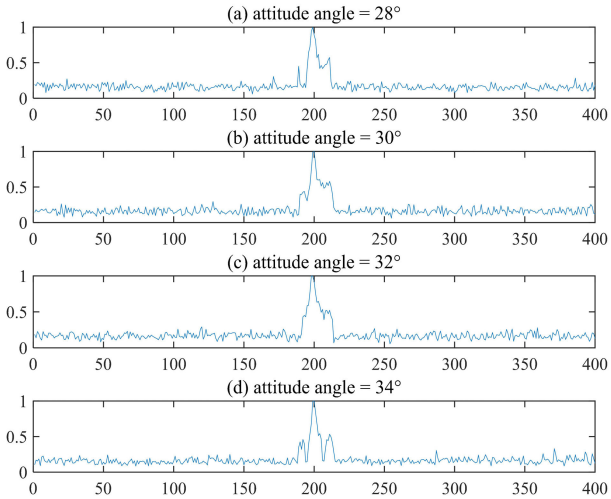

FIGURE 2. High sensitivity to aspect angles in HRRP signals. (a-d) Denote the same target in different aspect angles. Large variances among different aspect angles can be observed.

features will decrease, limiting the final HRRP recognition performance.

Therefore, a deep transfer learning framework is proposed in this paper to address the HRRP recognition problem when the training data have incomplete aspect angles. The task can be considered as an ill-posed pattern recognition problem, and it is natural to introduce additional prior information to alleviate this problem. The proposed work is motivated by the following assumptions: sometimes, the HRRP data of certain targets that cover all the aspect angles are available, for example, HRRP signals simulated from mathematical calculation or an HRRP collected from cooperative targets. There should be some hidden information that can be explored in these auxiliary HRRP signals. This study explores and transfers the information or knowledge from the auxiliary data to reduce the ill-posedness of the proposed task.

Transfer learning aims to transfer knowledge from the auxiliary source domain to improve the performance in the target domain [20]. The proposed work introduces additional auxiliary HRRP datasets with complete aspect angles as the source domain. Thus, the discriminative patterns are explored as knowledge and then transferred to the target domain to improve the recognition performance in a deep inductive network. Furthermore, a deep domain adaptation network is used to enforce the intraclass consistency, which can be considered as transferring additional knowledge from the auxiliary dataset to enhance the performance in the proposed task.

The main contributions of this paper can be summarized as follows:

1) To the best of the authors' knowledge, this is the first work to contribute to HRRP target recognition with incomplete aspect angle training data.

2) Motivated by the application scenarios, the proposed work introduces an auxiliary dataset with complete aspect angle HRRP signals as the source domain. A deep inductive

transfer learning framework is used to enhance the recognition performance by introducing additional knowledge from the source domain.

3) The proposed work further considers the intraclass consistency in the auxiliary dataset by introducing a deep domain adaptation network to benefit the recognition task by reducing the sensitivity to the aspect angles of the HRRP signals.

The remainder of this paper is organized as follows: The proposed framework is described in Section II. The HRRP data simulation and the experimental results are discussed in Section III. Related discussion is provided in Section IV. Finally, the proposed work is concluded in Section V.

II. THE PROPOSED METHOD

A. HRRP DATA FORMULATION

As stated in the introduction, an HRRP signal is the vector sum of a radar echo projected on a ray, and its resolution is inversely proportional to the radar bandwidth Δr. Therefore, an HRRP signal with a higher resolution can be obtained by using wide-band radar [17]. In the direction of the radar line of sight, the target is equivalent to a number of distance units of width Δr. The echo of each distance unit is the sum of the echoes of all the scattering centers in the unit. The ith echo is defined as follows:

$$\begin{aligned} x(i) &= \Psi_i(f) \\ &= \sum_{k=1}^{N_i} a_{i,k} exp(j2\pi f \tau_{i,k}) \\ &= I(i) + jQ(i) \end{aligned} \tag{1}$$

where N_i represents the number of target scattering centers in the ith distance unit; $a_{i,k}$ is the scattering intensity of the kth scattering center in the ith distance unit, which also includes the shape and the structure information of the target; and $\tau_{i,k}$ is the arrival time of the kth scattering center in the ith distance unit, which is determined by the distance from the scattering center to the origin of the radar coordinates. $I(i)$ and $Q(i)$ represents the real and imaginary parts of the signal, respectively.

In practical applications, the RATR technique usually chooses the amplitude range image for target recognition since the phase distance image is highly sensitive to the aspect angle and the distance of the target. The expression is as follows:

$$\begin{aligned} x &= [|x(1)|, |x(2)|, |x(3)|, \ldots, |x(n)|]^T \\ &= [\sqrt{I(1)^2 + Q(1)^2}, \sqrt{I(2)^2 + Q(2)^2}, \\ &\quad \ldots, \sqrt{I(n)^2 + Q(n)^2}]^T \end{aligned} \tag{2}$$

where n is the dimension of the HRRP signal. The RATR technique also adopts some preprocessing methods, such as center alignment and amplitude normalization, to overcome the time-shift and amplitude sensitivity.

B. BASIC CONCEPTS OF TRANSFER LEARNING

Domains and tasks are the two basic concepts in transfer learning. There are two domains in transfer learning:

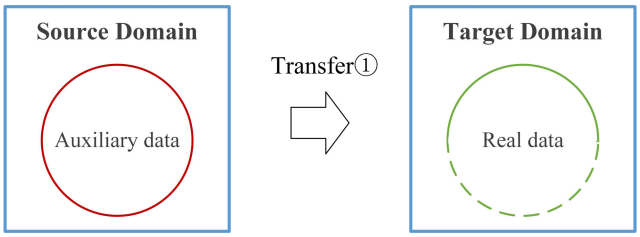

FIGURE 3. Definitions of source and target domains in HRRP recognition with deep inductive transfer learning. The dashed and the solid lines denote the uncaptured and the captured aspect angles, respectively. The auxiliary data in the source domain cover all the possible aspect angles while the real data only cover a portion.

$D_s = \{(x_1^{(s)}, y_1^{(s)}), \ldots, (x_n^{(s)}, y_n^{(s)})\}$ and $D_t = \{(x_1^{(t)}, y_1^{(t)}), \ldots, (x_n^{(t)}, y_n^{(t)})\}$ denote the source and target domains, respectively, with the corresponding tasks T_s and T_t. Transfer learning aims to reduce the generalization error of the target domain prediction model $f_t(x)$ under the condition of $D_s \neq D_t$ or $T_s \neq T_t$ [20].

C. THE PROPOSED METHOD

1) DISCRIMINATIVE POWER TRANSFER VIA DEEP INDUCTIVE TRANSFER LEARNING

According to [20], inductive transfer learning has the following characteristics: the data in the source domain are fully labeled, while the data in the target domain are only partially labeled. Therefore, as shown in Figure 3, the auxiliary HRRP data with complete aspect angles are considered as the source domain, while the real data with incomplete aspect angles are considered as the target domain.

In the source domain, the HRRP signals are all available at each possible aspect angle, while in the target domain, the HRRP signals are only available at several aspect angles. Although both the feature space and the data distribution of the two domains are different, the discriminative patterns in the source domain can still be explored by training any typical CNN model with the complete-angled HRRP signals. Thus, the discriminative patterns are considered knowledge and can be transferred to the target domain.

The implementation steps are as follows:

1) Choose a 1-D CNN model, e.g. 1-D AlexNet;

2) Pretrain the network with auxiliary data in the source domain;

3) Fine-tune the network with the real data in the target domain.

It should be mentioned that the HRRP signals in the source domain are not assumed to have the same attributes as those in the target domain. For example, if the proposed task is to recognize categories among ships, the source domain can be simulated HRRP signals from aircrafts. This assumption effectively releases the burden of collecting sufficient data in the source domain.

2) INTRA-CLASS CONSISTENCY REGULARIZATION VIA DEEP TRANSDUCTIVE TRANSFER LEARNING

As described above, the HRRP signals have large variance across different aspect angles even when they belong to the

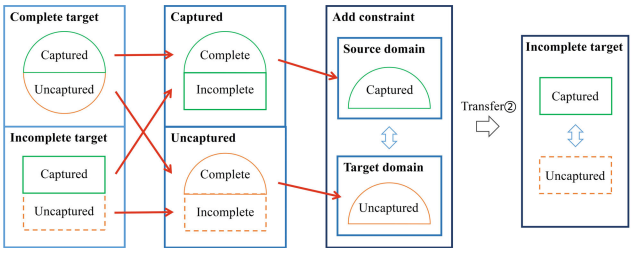

FIGURE 4. Definitions of source and target domains in HRRP recognition via deep transductive transfer learning. The circle and the rectangle denote the complete and the incomplete targets, respectively. The green and orange denote the captured and the uncaptured aspect angles, respectively. The dashed line denotes the unknown HRRP signals. The knowledge that is assumed to be transferred from the source domain to the target domain is the robust representative power between the captured and the uncaptured angles within the complete target.

same target. The high aspect-angle sensitivity results in a great challenge for feature extraction. The previous subsection aims to release this burden by introducing discriminative power from auxiliary data. This subsection explores the intraclass consistency to further improve the recognition performance. The idea is simple: if two HRRP vectors from different aspect angles belong to the same target, they are assumed to have the same discriminative pattern in the classifier, although the variance in their appearance is large. Thus, it is natural to consider enforcing the intraclass consistency in the proposed recognition task.

Similar to the previous subsection, an auxiliary dataset is introduced and used to explicitly explore the intraclass consistency. This auxiliary dataset is assumed to be real HRRP signals with complete aspect angles, and the intraclass consistency is considered knowledge and can be transferred into real HRRP signals with incomplete aspect angles. Therefore, the idea of domain adaptation, a branch of transductive transfer learning, is employed in the proposed work to improve the performance by suppressing the aspect-angle sensitivity.

There are two types of targets in the proposed method: complete targets with complete HRRP aspect angles and incomplete targets that only have part of the aspect angles. Moreover, there are two types of HRRP signals: those from captured angles and those from uncaptured angles. Figure 4 provides the definitions of the source and target domains. The HRRP signals from the captured and uncaptured aspect angles of the complete targets are both available, while the HRRP signals from uncaptured aspect angles of the incomplete targets are unavailable. Unlike the definition in the previous stage, the HRRP signals from the captured and uncaptured aspect angles from complete targets are defined as the source and target domains, respectively.

The intraclass or intratarget consistency is enforced by introducing a regularization term to the CNN network for feature extraction. This term aims to minimize the distribution distances between the captured and uncaptured angle data features in the complete target to simultaneously emphasize the robustness and representative power of the extracted features.

The proposed work chooses the maximum mean discrepancy (MMD) as the regularization term between the two domains. The main function of the MMD is to measure the similarity between two distributions. Given the two distributions p and q, a continuous function f, their sample space is found so that the mean value of the mapping difference between the samples in the two distributions is maximized, this mean value of the difference is called the MMD distance, which can reflect the similarity of the two distributions. The MMD distance is defined as:

$$MMD(p, q) = max|E_p[f(x)] - E_q[f(y)]| \tag{3}$$

where x and y represent the two samples of the two distributions and E represents the expected mean of the mapping. Now, the loss function of the proposed work can be defined as:

$$L_{ALL} = L_{CNN}((X_{SC}, Y_{SC}), (X_{TC}, Y_{TC}), (X_{SI}, Y_{SI})) + MMD(X_{SC}, X_{TC})) \tag{4}$$

where L_{ALL} is the loss function of any typical 1-D CNN network, X_{SC} and X_{TC} denote the HRRP signals of complete targets in the source and target domains, respectively; X_{SI} denotes the captured HRRP signals of incomplete targets; and Y_{SC}, Y_{TC} and Y_{SI} are their corresponding labels.

The second term in eq.(4) regulates the loss function by introducing the intraclass consistency from complete targets in an unsupervised manner, thus suppressing the aspect-angle sensitivity. Details are available in Algorithm 1.

Algorithm 1 Training Process of Transductive Transfer Learning

Input: Training HRRP samples $X = \{X_{SC}, X_{TC}, X_{SI}\}$, and all their labels $Y = \{Y_{SC}, Y_{TC}, Y_{SI}\}$; randomly initialize model parameters θ, learning rate l_r;

1: **for** number of training iterations **do**
2: Input X_{SC}, X_{TC}, X_{SI} as training samples;
3: Define $f_{last}(x)$ as the output feature of training batch x, obtain $f_{last}(X_{SC})$ and $f_{last}(X_{TC})$, then calculate their MMD value according to eq.(3);
4: Calculate L_{ALL} and the gradient of parameters Δ_θ;
5: Update $\theta^{i+1} = \theta^i + l_r \Delta_\theta L_{ALL}$;
6: **end for**

Output: The model for HRRP recognition.

III. EXPERIMENTS

A. HRRP DATA SIMULATIONS

Since real HRRP data are difficult to collect, this work generates simulated HRRP signals from SAR images by following the work of Gross *et al.* [21]. A public SAR dataset called MSTAR was selected as the HRRP dataset. There are seven types of ground targets in MSTAR: infantry fighting vehicles (BMP2_SN_9563), armored transport vehicles

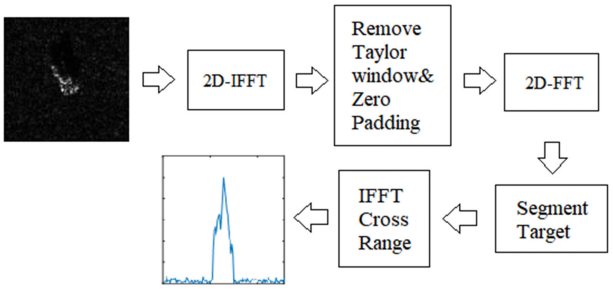

FIGURE 5. Flowchart to generate simulated HRRP signals [21].

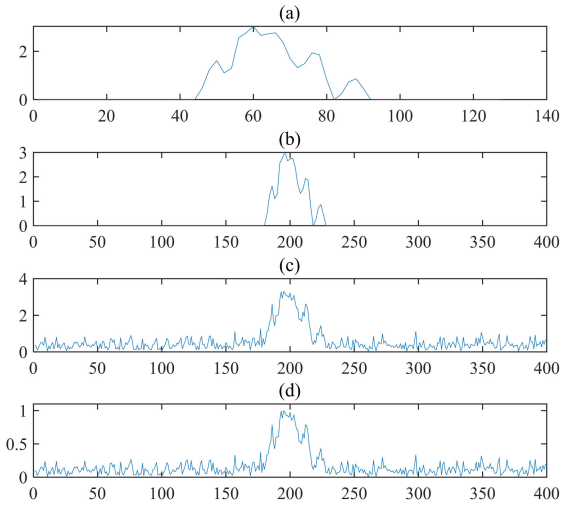

FIGURE 6. An example of HRRP data preprocessing. (a) Is the original HRRP signal calculated by SAR image stimulation; (b) is HRRP signal after size normalization; (c) is the signal after adding Gamma noise; and (d) is the signal after intra-frame normalization.

(BTR70_SN_C71), tanks (T72_SN_132), armored reconnaissance vehicles (BRDM_2), cargo trucks (ZIL131), self-propelled artillery (ZSU_234), and armored transport vehicles (BTR_60). Each category has two pitch angles (15, 17) and 180 aspect angles (1-180). As shown in Figure 5, the specific operation flow is as follows:

1) Perform a two-dimensional inverse Fourier transform (2D-IFFT) on the SAR image to obtain the echo phase history;

2) Deconvolute the 2D-IFFT transformed data to eliminate the influence of the Taylor window during the imaging process, that is, window removal;

3) Perform a two-dimensional Fourier transform (2D-FFT) to obtain an image after removing the window;

4) Perform target region segmentation on the processed image, first determine a suitable threshold of the grayscale image using Otsu's method, and then use this threshold to obtain the binary image;

5) Perform an inverse Fourier transform in the aspect direction to obtain a discrete frequency domain sequence in each direction, and then take the average value as the HRRP sequence.

An example of a simulated HRRP signal is shown in Figure 6(a).

B. PRE-PROCESSING

Due to the nonuniformity of the simulated HRRP dimension, the small amount of data and its amplitude sensitivity, a data preprocessing step was required as follows:

First, each HRRP vector was unified to the same size of 1*401 by performing zero-padding at both sides;

Second, the samples were augmented 10 times by adding gamma noise of the form $Noise = \sum_{i=1}^{b}[-\frac{1}{a}log(1 - U(1, 401))]$, in which $a = 60$, $b = 2$, and U stands for 401 dimensional uniform distribution between 0 and 1. After adding noise, the average SNR of the data used in the experiment is 11.14.

Third, intraframe normalization was performed, which is defined as follows:

$$x' = \frac{x - average(min5(x))}{average(max5(x)) - average(min5(x))} \tag{5}$$

where x and x' denote the HRRP signals before and after normalization, $max5()$ and $min5()$ denote the five maximum and minimum values in the signal, respectively, and $average()$ denotes the average operation.

This improved normalization strategy can avoid the instability problem caused by traditional linear normalization, such as the maximum being too large or the minimum being too small. The preprocessing steps are shown in Figure 6.

C. EXPERIMENTAL SETTINGS

The proposed task randomly selects three targets as experimental categories: infantry fighting vehicles (BMP2_SN_9563), armored transport vehicles (BTR70_SN_C71), and tanks (T72_SN_132), with category labels of 1, 2, and 3, respectively, and the remaining four categories are employed as auxiliary targets. More details are available in Table 1. Thus, the recognition task is defined as a three-class classification problem. Each category has two angle of pitch angles (15, 17) and 180 aspect angles (1-180) after preprocessing.

Following the previous definitions, there are complete and incomplete targets. Here, Category 1 is assigned as a complete target, which has HRRP signals with complete aspect angles in the training data. Categories 2 and 3 are assigned as incomplete targets, both of which have HRRP signals only from captured aspect angles in the training data.

Moreover, for incomplete targets, the captured and uncaptured aspect angles are defined by different sampling methods. There are two types of sampling methods in the following experiments: sparse sampling and continuous sampling. Continuous sampling refers to the continuous selection of partial angles as the captured aspect angles and the rest as the uncaptured aspect angles, while sparse sampling refers to uniformly sampling the selected angles as the captured aspect angles at two-degree intervals in the full-aspect domain, as shown in Figure 7.

The training and the testing sets in the experiments are shown in Table 2, where $X_{captured}$ and $X_{uncaptured}$ represent the captured and uncaptured aspect angles, respectively. For example, $X_{captured1}$ represents the captured aspect angles

TABLE 1. Data descriptions of the proposed three-class classification task.

Target	Category	Dimension	Attitude-angle	Pitch angle	Amount
infantry fighting vehicles	1	1*401	1-180	15	9750
				17	11640
armored transport vehicles	2			15	9800
				17	11640
tanks	3			15	9800
				17	11590
armored reconnaissance vehicles	4			17	14845
cargo trucks	5				14895
self-propelled artillery	6				14895
armored transport vehicles	7				12745

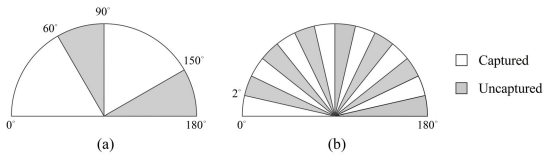

FIGURE 7. Captured and uncaptured aspect angles defined by two different sampling manners: (a) continuous sampling and (b) sparse sampling.

TABLE 2. Training and test sets in the experiment.

Training set	Test set
$X_{captured1}$, $X_{uncaptured1}$, $X_{captured2}$, $X_{captured3}$	$X_{uncaptured2}$, $X_{uncaptured3}$

in Category 1. The captured and the uncaptured angles of Category 1 were both used for training. Category 2 and Category 3 were incomplete targets; therefore, only their captured aspect-angle data were used for training.

D. IMPLEMENTATION DETAILS

The focus of the proposed work is to introduce two transfer learning methods to address the HRRP recognition problem with limited training data, and a typical CNN model was selected as the backbone, which is shown in Figure 8. The basic CNN model structure includes five convolutional layers and three fully connected layers (including a classifier). The max pooling operation was performed between each of the two convolutional layers, and the last fully connected layer integrates all the features and outputs the classification results. This network was modeled after AlexNet [22].

As mentioned previously, the four remaining categories (BRDM_2, ZIL131, ZSU_234, and BTR_60) are employed as auxiliary data.

The training steps of the proposed inductive transfer learning are as follows:

(a) Pretrain a four-category classifier with auxiliary data on this network;

(b) Replace the four neurons in the last layer of the network with three neurons

(c) Fine-tune the network with the training set in Table 2.

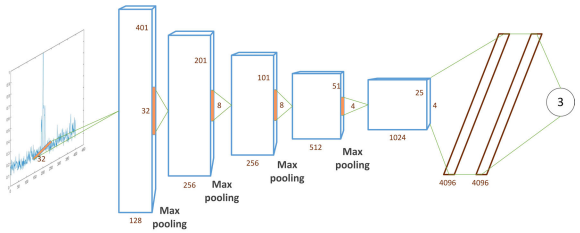

FIGURE 8. The architecture of the backbone in the proposed work. The blue square represents the dimension of the data stream in each convolutional layer. For example, in the first blue square, 401, 128 and 32 represent the dimension of the sample after the first convolution layer, the number of feature maps, and the size of the next layer's convolution kernels, respectively.

TABLE 3. The experimental results of the backbone with complete training data.

Pitch angle	Training sets	Test sets	Accuracy
15^o	19560	9790	99.49%
17^o	22700	12200	99.57%

For the recognition experiments with deep transductive transfer learning, the training loss is implemented by following eq.(4), where $X_{captured1}$ and $X_{uncaptured1}$ are employed to enforce the intratarget consistency. The MMD constraint is added at the second last and last layers of the network [23].

All the experiments were implemented in TensorFlow. The other configurations were as follows: the CPU was an Intel i7-7800X, the system memory was 64 GB, the graphics card was an NVIDIA GTX 1080 Ti, and the model had a batch size of 12 and a learning rate of 1e-4.

E. EXPERIMENTAL RESULTS

Before presenting the experimental results of the two proposed methods, the upper bound of the classification performance is demonstrated first, which is for the case in which the training set covers all possible aspect angles. For each pitch angle, two-thirds of the HRRP signals (C1-C3) are randomly selected as the training set, and the remaining signals are assigned as the testing set. The classification model's backbone is shown in Figure 8. As shown in Table 3, the accuracy of each pitch angle is above 99%, which indicates that the

TABLE 4. Accuracy comparisons of different methods.

Accuracy	Sparse sampling		Continuous sampling	
	pitch angle(15^o)	pitch angle (17^o)	pitch angle(15^o)	17 pitch angle (17^o)
Backbone	65.24%	63.79%	50.55%	49.37%
Backbone+Inductive	73.63%	69.74%	53.29%	56.49%
Proposed framework	78.51%	72.27%	54.57%	59.57%

TABLE 5. Average F1-score comparisons of different methods.

Average F-values	Sparse sampling		Continuous sampling	
	pitch angle(15^o)	pitch angle (17^o)	pitch angle(15^o)	17 pitch angle (17^o)
Backbone	0.7736	0.7280	0.6105	0.5886
Backbone+Inductive	0.8192	0.8065	0.6209	0.6749
Proposed framework	0.8410	0.8307	0.6318	0.6995

representative power of the backbone is significant when the training data cover all possible aspect angles.

The experimental results from the two proposed methods are reported in Tables 4 and 5, together with their baselines, which are the classification results from the backbone only and without any auxiliary training data. Moreover, the F1-score is also used as another validation indicator, which simultaneously takes the recall and precision into account.

First, the comparison of Tables 3 and 4 shows that the generalization performance of the backbone model of the basic network is significantly reduced in the proposed problem. This finding is mainly due to the large aspect-angle sensitivity of HRRP signals, as discussed previously. Thus, the features extracted by the baseline have limited representative power for the HRRP data from uncaptured aspect angles in the testing set.

Second, Tables 4 and 5 show the positive effect of the two transfer algorithms. The inductive transfer learning framework can improve the recognition performance in both sampling settings and for both pitch angles. The discriminative patterns can be explored by training the backbone on auxiliary data, which has HRRP signals from complete aspect angles. For example, the accuracy of auxiliary four-class recognition is 98.60%, which demonstrates the representative power of the extracted features. This information can be considered additional knowledge to be transferred to the proposed task to alleviate the ill-posedness. In view of network optimization, this pretraining method assigns the network a better initialization condition before training.

Transductive transfer learning introduces the MMD to constrain the difference between the aspect angle features, which can further improve the generalization performance of the network. The main reason for this result is that the regularization term narrows the feature distribution between the captured and uncaptured aspect angles in the complete targets. This regularization term can be considered as additional knowledge to suppress the negative effect of the aspect-angle sensitivity during the feature extraction procedure. In addition, the representative power, eq.(3) also emphasizes

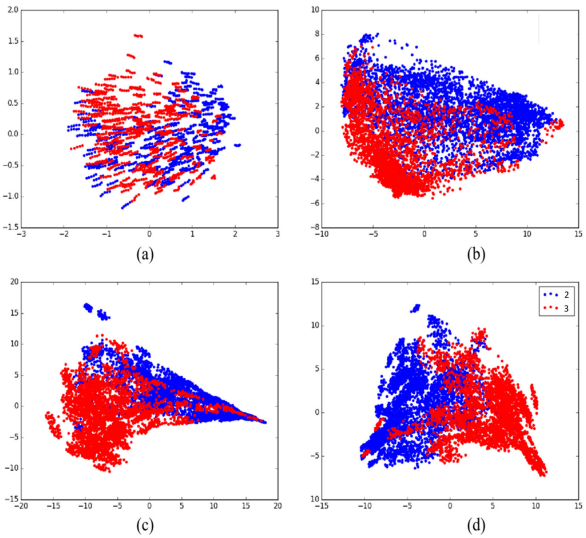

FIGURE 9. Discriminative power visualization via two-dimensional PCA analysis of sparse sampling in pitch angle 17. Feature distribution from (a) original data, (b) backbone model, (c) inductive transfer model, and (d) transductive transfer model.

the robustness of the extracted features across the aspect angles.

Furthermore, the accuracy in Tables 4 and 5 significantly declines during continuous sampling. The reasons for this phenomenon could be as follows: First, the differences and diversity of the samples increased due to the large span of the aspect angles. The range of the aspect angles from sparse sampling was small; however, the angle range from continuous sampling was large and continuous, and therefore, the characteristics learned by the network were only applicable to the data from the captured range. Thus, the robustness was poor. Second, the data used in the experiment that were obtained from SAR image inversion were unreal and inaccurate. There are some problems, such as amplitude shaking and the distortion of different angle features. Therefore, the accuracy of the data was low, which affected the experimental results.

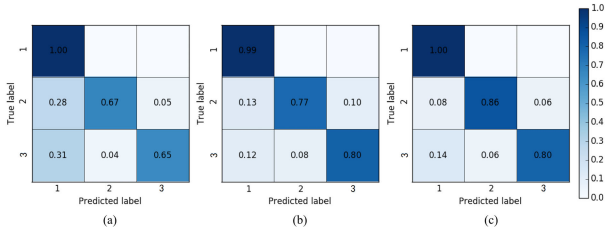

FIGURE 10. The confusion matrix results of 15 pitch angle sparse sampling. (a) Is the basic model, (b) is the inductive transfer model, and (c) is the transductive transfer model.

TABLE 6. Performance comparisons of different backbones.

Accuracy	Backbone only	Backbone+Inductive	Proposed framework
Propose backbone	65.24%	73.63%	78.51%
ResNet[18]	50.81%	59.12%	73.44%
DenseNet	58.17%	68.88%	70.93%

IV. RELATED DISCUSSIONS

The above experiments show that the two transfer algorithms proposed in this paper can alleviate the problem of data incompleteness to a certain extent. Thus, additional explorations were conducted from different evaluation aspects and with different network backbones.

First, for a more intuitive comparison, principal component analysis (PCA) was used for dimension reduction and to visualize the features. Figure 9 shows the PCA results for an experimental setup of 17 pitch angle sparse samplings, where 2 and 3 correspond to Category 2 and Category 3, respectively. The same conclusion can be observed from the PCA results. The pretrained inductive transfer learning algorithm has an obvious improvement, and the domain adaptive method based on MMD can further improve the generalization performance of the model for incomplete HRRP data.

Second, considering the differences between the three types of targets, this paper calculates the confusion matrix for the classification results of each model under the condition of the sparse sampling of 15 pitch angles.

Figure 10 shows that inductive transfer learning significantly improves the system's ability to identify the incomplete aspect angle of Category 2 and Category 3. Transductive transfer learning only improves the recognition performance of Category 2, which also verifies that the transductive transfer algorithm can improve the performance to a certain extent and that the network can enhance the feature learning power for incomplete targets. At the same time, since the uncaptured aspect angle data of Category 1 belonged to the training set, the recognition rate for Category 1 is close to 100%.

The proposed work provides a framework for HRRP recognition with limited aspect training data for the first time. The backbone in the work is almost the same as AlexNet, a typical CNN model. The proposed methods can be combined with any CNN model. To demonstrate the robustness across different backbones, the proposed backbone is also changed to other widely used CNN models. The experimental results are generated from HRRP signals with 15 pitch angles, and the sampling method is sparse sampling. ResNet and DenseNet are used to replace the backbone, as shown in Table 6. It can be observed from the experimental results that all the typical CNN frameworks improve, which supports the contributions of this paper. The table also compares the proposed framework with some of the latest works. For example, ResNet was used in [18] for HRRP recognition by introducing residual blocks in 1-D CNN models, and in this task,this backbone achieves a performance of 50.81% in the data used in this paper. With the proposed methods, the performance of ResNet dramatically increases to 73.44%. Thus, the proposed frameworks outperform latest reports.

V. CONCLUSION

CNNs demonstrate better recognition performance than the traditional scheme and other deep learning schemes in the complete-target HRRP dataset. To improve the recognition performance of incomplete targets, this paper introduces inductive and transductive transfer learning. A series of experiments show that the pretrained model can improve the data recognition rate of the incomplete target domain. In addition, adding constraints to the complete targets can further improve the recognition performance of the uncaptured aspect. This paper studies the problem of data loss in HRRP target recognition and proposes two effective deep transfer learning algorithms for the identification of incomplete targets. The proposed methods have practical application significance. An HRRP is one of the most widely used radar signal in the application of target recognition. In real-world scenarios, radar signals in other formats, e.g., SAR/ISAR, are also used as complementary evidence to support the final judgment.

REFERENCES

[1] P. Tait, *Introduction to Radar Target Recognition*, vol. 18. Edison, NJ, USA: IET, 2005.
[2] L. Du, H. Liu, and Z. Bao, "Radar HRRP statistical recognition: Parametric model and model selection," *IEEE Trans. Signal Process.*, vol. 56, no. 5, pp. 1931–1944, May 2008.
[3] L. Du, H. Liu, P. Wang, B. Feng, M. Pan, and Z. Bao, "Noise robust radar HRRP target recognition based on multitask factor analysis with small training data size," *IEEE Trans. Signal Process.*, vol. 60, no. 7, pp. 3546–3559, Jul. 2012.
[4] H.-W. Liu, B. Chen, B. Feng, and L. Du, "Radar high-resolution range profiles target recognition based on stable dictionary learning," *IET Radar, Sonar Navigat.*, vol. 10, no. 2, pp. 228–237, Feb. 2016.
[5] C. Du, B. Chen, B. Xu, D. Guo, and H. Liu, "Factorized discriminative conditional variational auto-encoder for radar HRRP target recognition," *Signal Process.*, vol. 158, pp. 176–189, May 2019.
[6] H. Zhang, D. Ding, Z. Fan, and R. Chen, "Adaptive neighborhood-preserving discriminant projection method for HRRP-based radar target recognition," *IEEE Antennas Wireless Propag. Lett.*, vol. 14, pp. 650–653, 2015.
[7] M. Pan, L. Du, P. Wang, H. Liu, and Z. Bao, "Noise-robust modification method for Gaussian-based models with application to radar HRRP recognition," *IEEE Geosci. Remote Sens. Lett.*, vol. 10, no. 3, pp. 558–562, May 2013.
[8] L. Du, H. He, L. Zhao, and P. Wang, "Noise robust radar HRRP target recognition based on scatterer matching algorithm," *IEEE Sensors J.*, vol. 16, no. 6, pp. 1743–1753, Mar. 2016.
[9] K. Simonyan and A. Zisserman, "Very deep convolutional networks for large-scale image recognition," 2014, *arXiv:1409.1556*. [Online]. Available: http://arxiv.org/abs/1409.1556

[10] C. Szegedy, W. Liu, Y. Jia, P. Sermanet, S. Reed, D. Anguelov, D. Erhan, V. Vanhoucke, and A. Rabinovich, "Going deeper with convolutions," in *Proc. IEEE Conf. Comput. Vis. Pattern Recognit. (CVPR)*, Jun. 2015, pp. 1–9.
[11] Z. Yun, T. Xuelian, L. Benyong, and W. Xueang, "Radar target recognition based on KLLE and a KNRD classifier," *WSEAS Trans. Signal Process.*, vol. 2, no. 6, pp. 47–57, 2010.
[12] L. Du, H. Liu, Z. Bao, and J. Zhang, "Radar automatic target recognition using complex high-resolution range profiles," *IET Radar, Sonar Navigat.*, vol. 1, no. 1, pp. 18–26, 2007.
[13] B. Feng, B. Chen, and H. Liu, "Radar HRRP target recognition with deep networks," *Pattern Recognit.*, vol. 61, pp. 379–393, Jan. 2017.
[14] B. Xu, B. Chen, J. Wan, H. Liu, and L. Jin, "Target-aware recurrent attentional network for radar HRRP target recognition," *Signal Process.*, vol. 155, pp. 268–280, Feb. 2019.
[15] Q. Zhang, J. Lu, T. Liu, P. Zhang, and Q. Liu, "Ship HRRP target recognition based on CNN and ELM," in *Proc. 4th Int. Conf. Electromechanical Control Technol. Transp. (ICECTT)*, Apr. 2019, pp. 124–128.
[16] J. Wan, B. Chen, B. Xu, H. Liu, and L. Jin, "Convolutional neural networks for radar HRRP target recognition and rejection," *EURASIP J. Adv. Signal Process.*, vol. 2019, no. 1, p. 5, Dec. 2019.
[17] K. Liao, J. Si, F. Zhu, and X. He, "Radar HRRP target recognition based on concatenated deep neural networks," *IEEE Access*, vol. 6, pp. 29211–29218, 2018.
[18] C. Guo, Y. He, H. Wang, T. Jian, and S. Sun, "Radar HRRP target recognition based on deep one-dimensional residual-inception network," *IEEE Access*, vol. 7, pp. 9191–9204, 2019.
[19] C. Zhao, X. He, J. Liang, T. Wang, and C. Huang, "Radar HRRP target recognition via semi-supervised multi-task deep network," *IEEE Access*, vol. 7, pp. 114788–114794, 2019.
[20] S. Jialin Pan and Q. Yang, "A survey on transfer learning," *IEEE Trans. Knowl. Data Eng.*, vol. 22, no. 10, pp. 1345–1359, Oct. 2010.
[21] D. C. Gross, M. W. Oppenheimer, B. Kahler, B. L. Keaffaber, and R. L. Williams, "Preliminary comparison of high-range resolution signatures of moving and stationary ground vehicles," *Proc. SPIE*, vol. 4727, pp. 205–213, Aug. 2002.
[22] A. Krizhevsky, I. Sutskever, and G. E. Hinton, "ImageNet classification with deep convolutional neural networks," in *Proc. Adv. Neural Inf. Process. Syst.*, 2012, pp. 1097–1105.
[23] M. Long, Y. Cao, J. Wang, and M. I. Jordan, "Learning transferable features with deep adaptation networks," 2015, *arXiv:1502.02791*. [Online]. Available: http://arxiv.org/abs/1502.02791

YI WEN received the B.S. degree from Xiamen University, Xiamen, China, in 2018, where she is currently pursuing the master's degree with the Department of Communication Engineering, School of Information Science and Engineering. Her main research interests include deep learning and signal processing.

LIANGCHAO SHI received the B.S. degree from Xiamen University, Xiamen, China, in 2018, where he is currently pursuing the master's degree with the Department of Communication Engineering, School of Information Science and Engineering. His main research interests include deep learning and signal processing.

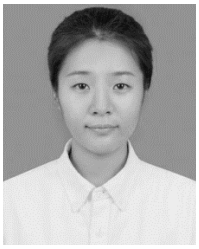

XIAN YU received the B.S. degree from Xiamen University, Xiamen, China, in 2016, and the master's degree from the Department of Communication Engineering, School of Information Science and Engineering, Xiamen University. Her main research interests include machine learning and image processing.

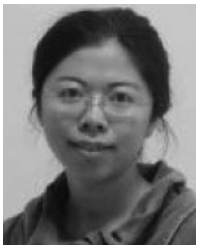

YUE HUANG received the B.S. degree from Xiamen University, Xiamen, China, in 2005, and the Ph.D. degree from Tsinghua University, Beijing, China, in 2010. She was a Visiting Scholar with Carnegie Mellon University, from 2015 to 2016. She is currently an Associate Professor with the Department of Communication Engineering, School of Information Science and Engineering, Xiamen University. Her main research interests include machine learning and image processing.

XINGHAO DING was born in Hefei, China, in 1977. He received the B.S. and Ph.D. degrees from the Hefei University of Technology, Hefei, in 1998 and 2003, respectively. From 2009 to 2011, he was a Postdoctoral Researcher with the Department of Electrical and Computer Engineering, Pratt School of Engineering, Duke University, Durham, NC, USA. Since 2011, he has been a Professor with the Department of Communication Engineering, School of Information Science and Engineering, Xiamen University, Xiamen, China. His main research interests include image processing and machine learning.